Res Chem Intermed (2017) 43:2891–2904
DOI 10.1007/s11164-016-2801-7

Synthesis of hierarchical porous carbon-TiO_2 composites as anode materials for high performance lithium ion batteries

Hui Zou[1,2] · Kang Yan[1,2] · Ye Cong[1,2] · Xuanke Li[1,2] · Jiang Zhang[2] · Zhengwei Cui[2] · Zhijun Dong[2] · Guanming Yuan[2] · Yanjun Li[2]

Received: 5 September 2016 / Accepted: 31 October 2016 / Published online: 30 November 2016
© Springer Science+Business Media Dordrecht 2016

Abstract Hierarchical porous carbon-TiO_2 composites have been successfully synthesized via evaporation-induced self-assembly and in situ crystallization. The titania content and calcination temperature play significant roles in the structures, pore textures (micropore and mesopore) and electrochemical properties. The prepared composites as anode materials for lithium ion batteries show superior discharge capacity, cycling performance and rate capability. The composite of HPCT-600-5 exhibits the highest reversible capacity of 376.9 mAh g^{-1} after 50 cycles at a rate of 0.1 C, and retains the capacity of 240.5, 180.2 and 117.0 mAh g^{-1} even at the higher rates of 0.5, 1 and 2 C, respectively (1 C = 350 mA g^{-1}). This outstanding electrochemical performance is attributed to the synergistic effects of hierarchical porous carbon and titania due to the unique structures, such as higher specific surface area and pore volume, fine TiO_2 particles, appropriate distribution of hierarchical pore size and optimum content of TiO_2. The special structures of the composites can improve the wettability of the electrolyte, provide a large storage space for the Li ion, enhance the initial charge–discharge efficiency and reduce the resistance of the charge transfer and the diffusion of Li ions.

Keywords Hierarchical pores · Carbon/TiO_2 composites · Synergistic effect · Anode · Lithium ion battery

✉ Ye Cong
congye@wust.edu.cn

✉ Xuanke Li
xkli8524@sina.com

[1] The State Key Laboratory of Refractories and Metallurgy, Wuhan University of Science and Technology, Wuhan 430081, Hubei, People's Republic of China

[2] The Hubei Province Key Laboratory of Coal Conversion and New Carbon Materials, Wuhan University of Science and Technology, Wuhan 430081, Hubei, People's Republic of China

Introduction

Lithium ion batteries (LIBs) have been widely used in portable electronic devices such as cellular phones, camcorders, and notebook computers due to their high energy density, long life cycle, no memory effect and low toxicity [1–3]. However, with the development of LIBs in the fields of various types of electrical vehicles (EVs) and energy storage for utility grids, it has been a harsh demand on advanced anode materials with high energy density, high power density, and long-term cycle stability.

Among anode materials, Titania (TiO_2) has been considered as a potential candidate for LIBs because of its better accommodation of mechanical strain, low volume change (<4% for Li_xTiO_2, $0 \leq x \leq 1$) [4, 5] during charging/discharging, good cycling performance, low cost and being environmentally friendly [6–10]. TiO_2 offers a theoretical capacity of 335 mAh g^{-1} based on the complete reduction of Ti^{4+} to Ti^{3+}. However, the practical capacity of TiO_2 anodes is only 168 mAh $g^{-1,}$ and the rate capacity is not ideal due to the poor electronic conductivity and low Li ion diffusion coefficient [11–13]. One commonly used approach to enhance the electrochemical performance is to shorten the Li ion diffusion distance and increase the contact area with the electrolyte, such as fabrication of mesoporous and hollow structures, nanoparticles and nanosheets TiO_2 [14, 15]. Xiu et al. [16] prepared mesoporous anatase TiO_2 with a disk-like morphology by direct pyrolysis of a titanium metal–organic framework [MIL-125(Ti)] in air. The as-prepared TiO_2 as an anode material shows superior high-rate performance and excellent electrochemical stability, attributed to the unique mesoporous structure. Zhang et al. [17] have reported flowerlike hydrogenated TiO_2(B) nanostructures via a facile solvothermal approach combined with hydrogenation treatment. The hydrogenated TiO_2(B) nanostructures exhibit improved lithium ion storage performance including higher specific capacity, superior rate performance and better cycling stability.

Carbon materials are widely used as the anode materials of lithium-ion batteries due to their unique structure and performance characteristics. The composite of nano-TiO_2/activated carbon was prepared by hydrolytic precipitation of TiO_2 from $TiCl_4$ in a mixed aqueous solution containing activated carbon [18]. Chen et al. [19] reported on the design and synthesis of a novel hybrid nanoarchitecture of carbon nano-tubes (CNTs) coated with TiO_2-B nanosheet arrays. The resultant hybrid composites showed high reversible capacity and superior rate capability for LIB applications. Ge et al. [20] prepared carbon coated TiO_2 particles, which presented higher specific capacity and better capacity retention than the untreated TiO_2 particles. Lee et al. [21] fabricated porous carbon/TiO_2 composites through polymerization-induced phase separation and use as an anode for Na-ion batteries. Zhang et al. [22] had successfully prepared TiO_2/carbon hollow spheres using a template method. The composite anode delivered a high specific capacity of 140.4 mAh g^{-1} over 100 cycles under 100 mA g^{-1}, and showed remarkable rate performance.

In recent years, it has been extensively accepted that hierarchy in pore sizes can permit better permeation of an electrode through a porous electrode. Hierarchical porous structures are of benefit for improving both specific capacity and rate capability of the energy storage materials. For a lithium ion battery, the mesopores can provide high pore volume to enhance the electrolyte diffusion, and the micropores can increase the surface area and active sites to enhance the Li ion storage [23–25]. Cheng's group reported a 3-D aperiodic hierarchical porous graphitic carbon (HPGC) as a promising electrode material for high-rate electrochemical capacitors [26]. The macropores can minimize the diffusion distances to the interior surfaces, and the mesoporous walls can provide low-resistant pathways for the ions through the porous particles. The micropores strengthen the electric-double-layer capacitance. Yushin and coworkers prepared carbide-derived carbons with combined miro- and meso-pores [23]. This material is a highly attractive host structure for the active material in lithium-sulfur battery cathodes with good rate performance and stability. $Li_4Ti_5O_{12}$/hierarchical porous carbon matrixes composites were prepared using a soluble polymers assisted sol–gel methodology with subsequent calcination and carbonization. The composites manifest high rate capacity and outstanding cycling stability.

In this study, we combined the advantages of TiO_2 and porous carbon to synthesize the hierarchical porous carbon-TiO_2 composites for LIBs application. The low-molecular-weight soluble phenolic resin, tetrabutyl titanate (TBT) and triblock copolymer F127 were employed as the carbon precursor, inorganic precursor, and structure-directing agent, respectively. The carbon component of the HPCT composites can improve the electronic conductivity and the hierarchical porous structure facilitates the Li-ion transport and increases the storage of Li ions. The intrinsic structure of titania is beneficial for reacting with lithium ions to form Li_xTiO_2. Therefore, the prepared composites show superior discharge capacity, cycling stability and rate performance compared with single TiO_2 or porous carbon.

Experimental

Preparation of the resol precursors

The resol precursor, a low molecular weight and soluble phenolic resin, was prepared using phenol and formaldehyde as reactant and sodium hydroxide (NaOH) as catalyst according to a method found in the literature[27]. In a typical procedure, 0.61 g of phenol was melted at 40–42 °C in a flask and mixed with 0.13 g of 20 wt% NaOH aqueous solution under stirring. After 10 min, 1.05 g of formalin (37 wt%) was added dropwise below 50 °C. Upon further stirring for 1 h at 70–75 °C, the mixture was cooled to room temperature, and the pH value was adjusted to about 7.0 by HCl solution. After water was removed by vacuum evaporation below 50 °C, separating sodium chloride as a precipitate at the same time, the final product was dissolved in ethanol (20 wt% ethanolic solution).

Synthesis of the HPCT composites

The HPCT composites samples were synthesized using resol precursor as carbon source, TBT as titanium source and triblock copolymer F127 as the template. First, 1.0 g of F127 was dissolved in 10 mL of ethanol and mixed with 10.0 g of resol precursor ethanol solution to obtain a homogeneous solution, which was named as solution A. Then 1.6 g of block copolymer F127 was dissolved in the mixture of 16 mL of ethanol and 1.0 mL of 2.0 M HCl and further stirred at 40 °C for 30 min. Then, a certain amount of TBT dissolved in 10 mL of ethanol was added to the obtained solution B. After homogeneously mixing the solution A and solution B, the obtained mixture was transferred into dishes and kept at room temperature for 8 h to evaporate ethanol. Subsequently, the mixture was thermopolymerized in an oven at 100 °C for 24 h. The as-made products were calcined in a tubular furnace at 350 °C for 3 h and followed at higher temperature (600–900 °C) for 2 h under Ar atmosphere, with a heating rate of 1 °C/min. The final products of hierarchical porous carbon-TiO_2 (HPCT) composites were denoted as HPCT-*T*-*x*, where *T* was the calcination temperature (600, 700, 800, and 900 °C) and *x* represented the amount of TBT (0, 2.5, 5, 7.5, 10 mmol). HPCT-600-T (namely pure titania) was prepared by the same process with 10 mmol TBT in solution B and without resol precursors and calcined at 600 °C. The general synthesis process of the hierarchical porous carbon-TiO_2 composite is shown in Scheme 1.

Characterization of the composites

The crystal structures of the samples were characterized via X-ray diffraction (XRD) using a XPert PRO MPD with filtered Cu Ka radiation ($\lambda = 1.54056$ Å) at 40 kV. The diffraction patterns were collected at room temperature by step scanning in the range of 10°–90° at a scan rate of 5°/min. The microstructures of the synthesized products were observed by transmission electron microscope (TEM) JEM-2100. The morphology of the samples was analyzed by scanning electron microscopy (SEM, Helios Nanolab 600i). N_2 adsorption–desorption isotherms were collected at 77 K on a surface area and porosity analyzer (Micrometrics ASAP 2020). Using the Barrett–Joyner–Halenda model, the pore size distribution in the mesopore range (>2 and <50 nm) was derived from the adsorption branch of the isotherms. Using the Horvath–Kawazoe (HK) model, the micropore distribution (<2 nm) was derived from the adsorption branch of the isotherms. The micropore

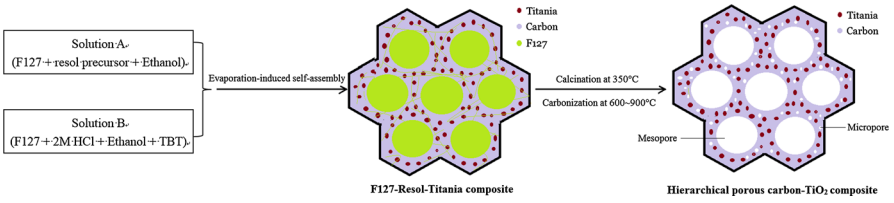

Scheme 1 The synthesis process of the hierarchical porous carbon-TiO_2 composite

surface areas were calculated from the *t*-plot method. The total pore volumes (V_t) were estimated from the adsorbed amount at a relative pressure P/P_0 of 0.995.

Preparation of electrode and electrochemical measurements

The working electrodes were prepared by mixing active material (the as-prepared HPCT composites), conductive agent (carbon black) and polyvinylidene fluoride (PVDF) binder at a weight ratio of 85:5:10 in 1-Methyl-2-pyrrolidinone (NMP). The slurries of the above mixture were deposited onto copper foil current collectors (12 mm in diameter). Thereafter, the electrodes were dried at 60 °C for 24 h. Pure lithium metal foil was used as the counter-electrode. Also,1 M $LiPF_6$ in ethylene carbonate (EC)/dimethyl carbonate (DMC)/ethyl methyl carbonate (EMC) (EC:DMC:EMC = 1:1:1, volume ratio) was used as the electrolyte. The galvanostatic charge/discharge and rate performance were measured in a CR2016 coin-type cell using a NEWARE BTS-5V50 mA computer-controlled battery test station at a cutoff voltage of 0.005–3.0 V under current densities of 0.1, 0.5, 1 and 2 C (1 C = 350 mA g^{-1}). Electrochemical impedance spectroscopy (EIS) measurements were performed on the CHI 660D electrochemical workstation in the frequency range from 0.010 Hz to 100 kHz with a 5 mV amplitude.

Results and discussion

Structure and morphology characteristics of the hierarchical porous carbon-TiO_2 (HPCT) composites

XRD patterns of the HPCT-*T*-5 composites, calcined at different temperatures in argon with 5 mmol addition of TBT, are shown in Fig. 1a. With the increasing of calcination temperature, the diffraction peak of anatase ($2\theta = 25.3°$) grows gradually and the diffraction peak of rutile ($2\theta = 27.3°$) appears above 800 °C.

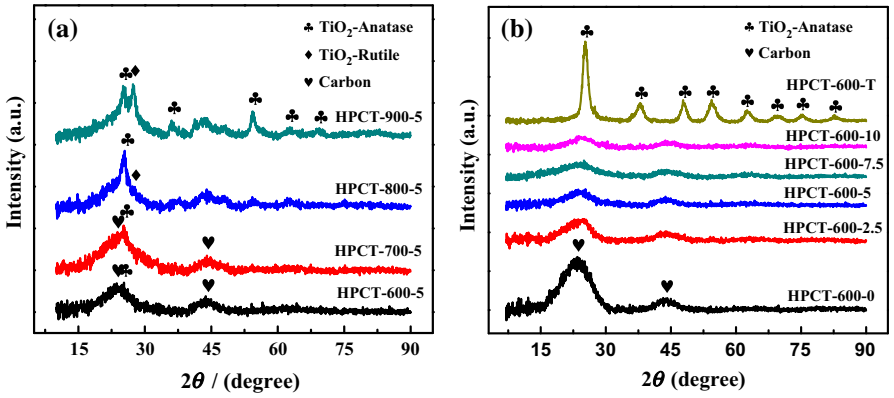

Fig. 1 XRD patterns of **a** the HPCT-*T*-5 and **b** the HPCT-600-*x* composites

Figure 1b shows the XRD patterns of the HPCT composites synthesized with various TBT additions and calcined at 600 °C in Ar (HPCT-600-*x*). Two broad diffraction peaks for HPCT-600-0 (namely hierarchical porous carbon) at $2\theta = 23°$ and 43° can be indexed as the (002) and (100) planes of carbon, implying a typical amorphous carbon structure [15]. Inversely, the HPCT-600-T (namely pure titania) shows the characteristic diffraction peaks at 25.3°, 37.9°, 48.4°, 53.9°, and 62.7°, which can be attributed to (101), (103), (200), (105), and (213) crystal planes of anatase TiO_2 (JCPDS 01-071-1167), respectively. However, the diffraction peaks of TiO_2 for HPCT-600-*x* ($x = 2.5$, 5, 7.5 and 10) are hardly identified in Fig. 1a, due to that titania is embedded into the frameworks of carbon, and the growth of titania grains is inhibited. These are helpful for avoiding the agglomeration of titania during the charge and discharge process. The titania contents of HPCT-600-2.5, HPCT-600-5, HPCT-600-7.5 and HPCT-600-10 are 18, 28, 36 and 40 wt% measured by TG analysis (not shown), respectively.

TEM analysis was performed to identify the morphology and structure. As shown in Fig. 2a, the ordered stripe-like 1-D channel can be clearly observed, indicating the nature of ordered mesoporous characteristics of HPC. Compared with HPC, the HPCT-600-5 keeps the stripe-like channels, and the structural ordering is partly destroyed, due to the growing TiO_2 nanocrystals thrust into the mesochannels from the walls and partly damage the well-organized structure. Unfortunately, it is hard to seek out the lattice fringes of titania in a HRTEM image (inset of Fig. 2b). This may be ascribed to that anatase has embedded into the frameworks of carbon and presents as being of the form of microcrystalline or amorphous, which is consistent with the results of XRD. Pure titania (HPCT-600-T) shows homogeneous particles

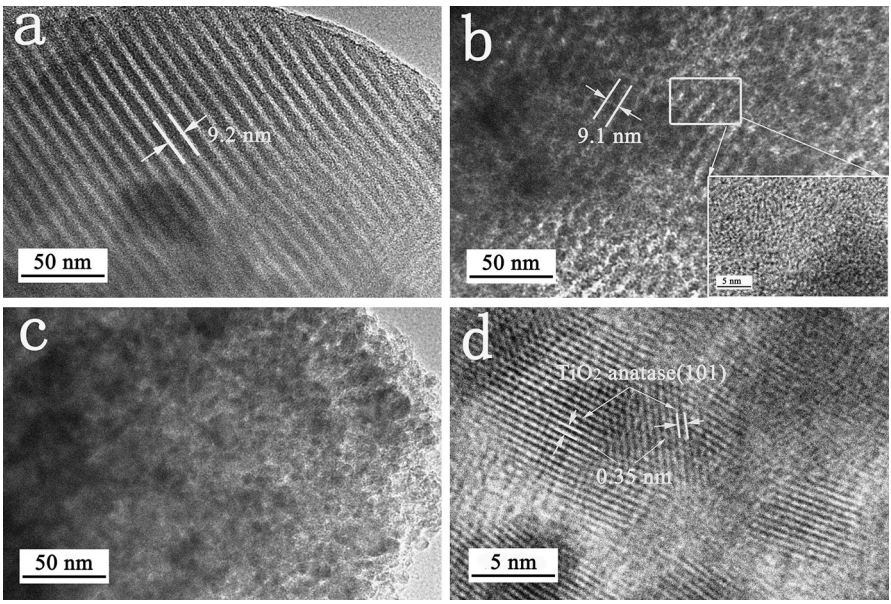

Fig. 2 TEM and HRTEM images of **a** HPCT-600-0, **b** HPCT-600-5, **c**, **d** HPCT-600-T

in Fig. 2c, and in the HRTEM image (Fig. 2d) which indicates the lattice spacing of 0.35 nm corresponding to the (101) plane of anatase.

Figure 3 presents the SEM images of the HPCT composites calcined at 600 °C with various TiO_2 contents. Uniform porous structure can be clearly observed in Fig. 2a. After incorporated with TiO_2, the 1-D channels still exist but the ordering degree decreases because of the embedding of TiO_2 nanoparticles into the walls and thrusting into the channels. For HPCT-600-5 (Fig. 3c), the content of titania increases and the ordering further decreases, which is in accordance with the TEM results. In addition, no evidently ordered pores can be found in the pure TiO_2 (HPCT-600-T).

Nitrogen adsorption/desorption measurement is a powerful technique to analysis the pore structure of the porous materials. As presented in Fig. 4a, the samples manifest the similar shapes and positions of the hysteresis. According to the International Union of Pure and Applied Chemistry (IUPAC) classification, the

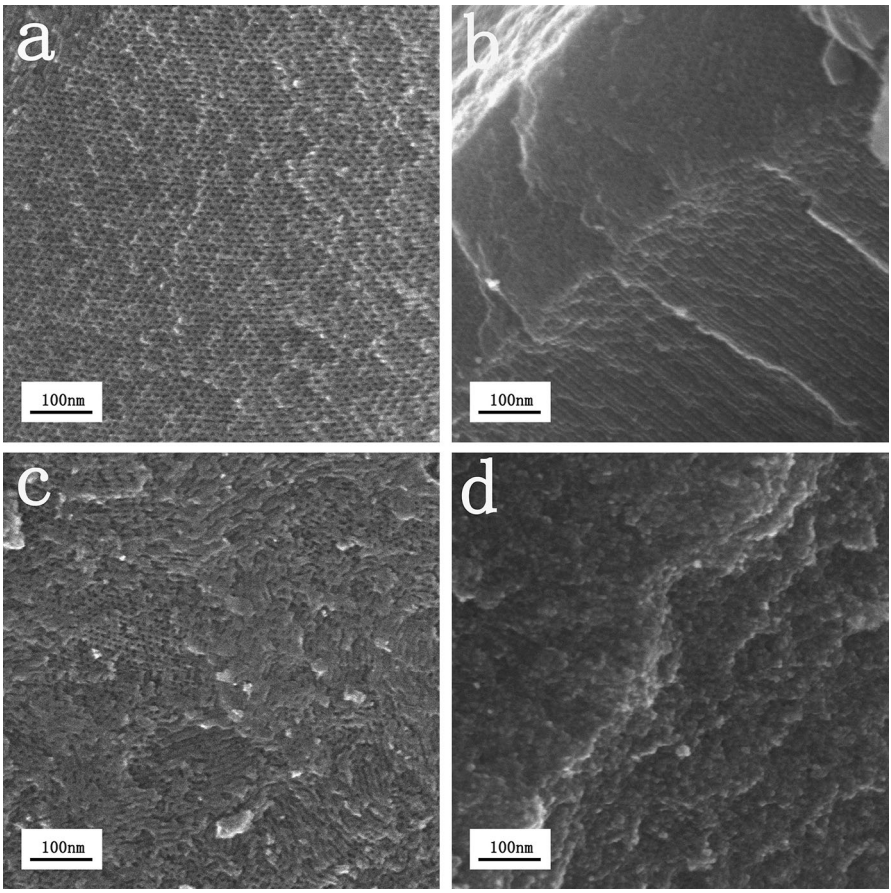

Fig. 3 SEM images of the HPCT-600-*x* composites. **a** HPCT-600-0, **b** HPCT-600-2.5, **c** HPCT-600-5 and **d** HPCT-600-T

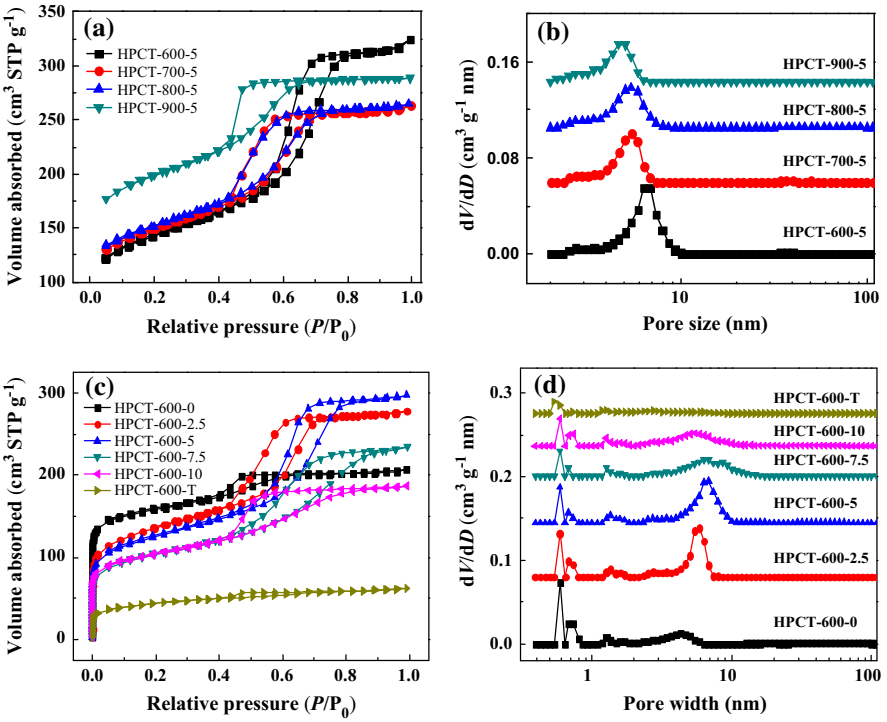

Fig. 4 N_2 adsorption/desorption isotherms of **a** HPCT-*T*-5 and **c** HPCT-600-*x*; and the pore size distributions of **b** HPCT-*T*-5 and **d** HPCT-600-*x*

isotherms are typical type IV curves with a distinct capillary condensation step and a H1 hysteresis loop in the middle P/P_0 range of 0.4–0.8 for the composites calcined at 600–800 °C. The mesopore size distributions are narrow in the range of 4–7 nm as shown in Fig. 4b. What is more, with the calcination temperature increasing, the specific surface areas increase and the pore size decreases (shown in Table 1; Fig. 4b). It is attributed to the shrinkage of the carbon skeleton [27].

As can be seen in Fig. 4c, all isotherms of the HPCT composites are a combination with type I and IV isotherms, with similar shapes and positions of the hysteresis. Volume absorbed value is increasing sharply when the relative pressure (P/P_0) around 0.01, demonstrating abundant microspores exist in the composite materials. The micropore diameters are centered at 0.5–0.6 nm as shown in PSD (Fig. 4d). Previous research has shown that micropore sizes <1 nm can be beneficial to enhance the electrochemical performance [28, 29]. Meanwhile, all the HPCTs indicate type IV isotherms with a notable capillary condensation step in the relative pressure (P/P_0) range of 0.45–0.80, explaining that mesoporous distribution of HPCTs. According to IUPAC classification, hysteresis loops are H1 type. It is notable that the hysteresis loop for HPCT-600-5 is at higher relative pressure, which suggests its larger mesopores size (shown in Fig. 4d). In addition, the D_{BJH} of HPCT-600-5 shows higher value. With the increase of the titania content, the

Table 1 Structural parameters of HPCT-600-*x*

Sample name	S_{BET} ($m^2\ g^{-1}$)	S_{micro} ($m^2\ g^{-1}$)	D_{BJH} (nm)	V_t ($cm^3\ g^{-1}$)	V_{micro} ($cm^3\ g^{-1}$)	V_{meso} ($cm^3\ g^{-1}$)	V_{meso}/V_t (%)	D_{HK} (nm)
HPCT-600-0	412.9	232.2	3.5	0.32	0.21	0.11	35.1	0.53
HPCT-600-2.5	386.0	108.5	4.8	0.43	0.16	0.27	63.0	0.56
HPCT-600-5	360.1	96.7	5.8	0.46	0.14	0.32	69.1	0.57
HPCT-600-7.5	308.4	87.5	5.9	0.36	0.13	0.24	64.4	0.56
HPCT-600-10	291.9	103.9	4.6	0.29	0.12	0.17	56.9	0.55
HPCT-600-T	121.7	24.7	3.7	0.10	0.05	0.05	49.0	0.59

S_{BET}, the specific surface areas calculated by the BET method; S_{micro} the micropore surface areas calculated by t-plot method; D_{BJH}, the average pore size by BJH mode; V_t the total pore volume; V_{micro}, the micropore volume by HK mode; D_{HK}, the micropore size by HK mode

specific surface areas of HPCT-600-*x* decrease while the total pore volume (V_t) and mesopore volume (V_{meso}) increases first and then decreases and reach the maximum value for HPCT-600-5. These results may be attributed that titania phase embedded into the frameworks of the carbonaceous matrix and inhibited the shrinkage of carbon skeleton as well. But the excess titania may thrust into and block part of the mesoporous channels to deduce the mesopore volume. The large pore size and volume cannot only guarantee adequately contact between electrode materials and electrolyte, but also facilitate the fast transport of lithium ions.

Electrochemical performance

The HPCT composites were used as active materials for Li ion half-cells to investigate the electrochemical performance. The first charge–discharge cycle profiles and the initial columbic efficiency of HPCT-T-5 at a current density of 35 mA g^{-1} (0.1 C) are shown in Fig. 5a, b, respectively. The charge/discharge capacities decrease with the increase of the calcination temperature. This may be due to the phase transformation of TiO_2 from anatase to rutile and the decrease of mesopore size (as shown in Fig. 4b). The initial columbic efficiency also decreases because of the higher specific surface area and increasing capacity loss for the formation of solid electrolyte interface (SEI) films.

The electrochemical performances of HPCTs calcined at 600 °C with different TiO_2 contents were evaluated. Figure 6a, b show the first charge–discharge specific capacities, the initial coulomb efficiencies and the insertion/extraction of Li ions of the HPCTs. These results clearly indicate that the HPCT composites have superior performance of Li ion insertion in the first charge–discharge process than the pure hierarchical porous carbon (HPCT-600-0) and the pure titania (HPCT-600-T), which are mainly attributed to the high specific surface area, pore volume especially

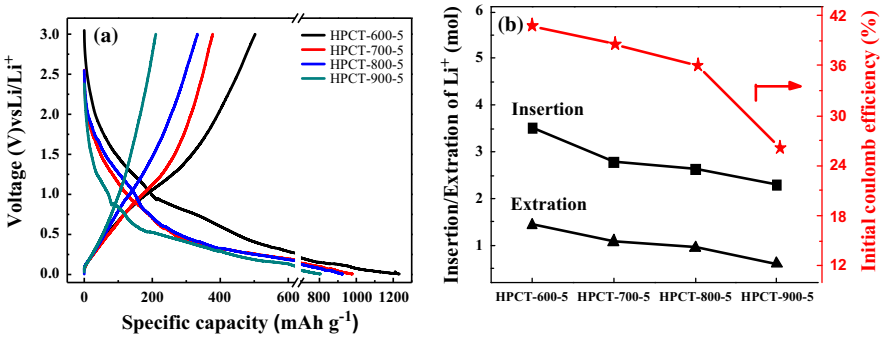

Fig. 5 **a** The first charge–discharge curves (at 0.1 C); **b** insertion/extraction of Li ions and initial coulomb efficiency of HPCT-*T*-5

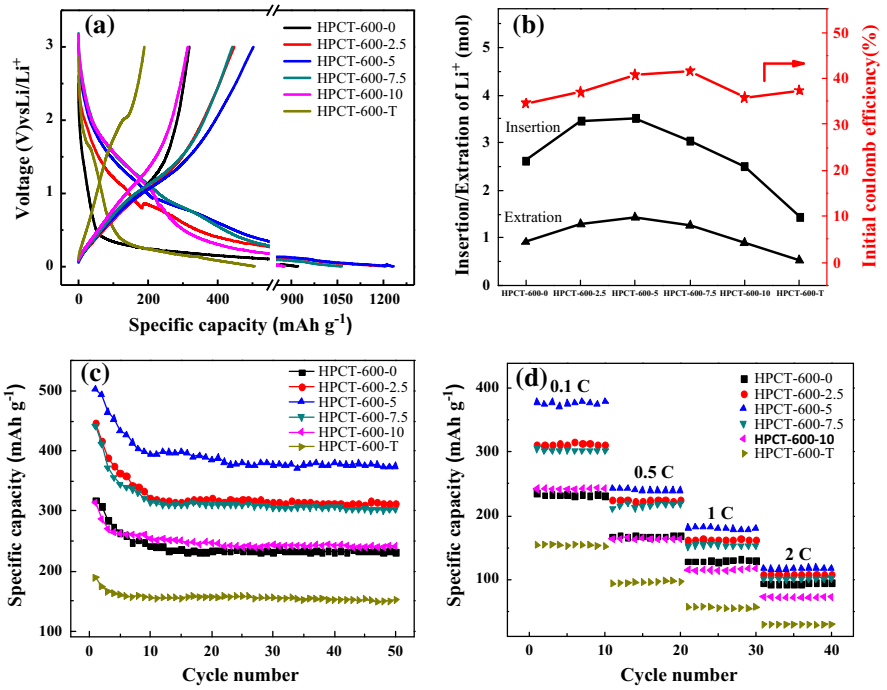

Fig. 6 **a** The first charge–discharge curves (at 0.1 C); **b** insertion/extraction of Li ions and initial coulomb efficiency at first cycle; **c** cycling performances (at 0.1 C); and **d** rate capabilities of HPCTs at 0.1, 0.5, 1 and 2 C, respectively

mesopore volume, and large pore size (Table 1). It is worth noting that the first charge and discharge capacities of HPCT-600-5 can reach 1232.8 and 502.5 mAh g^{-1}, respectively, which has already exceeded the theoretical values of titania and graphite. It may be related to the larger mesopore size and mesopore volume (Fig. 6b; Table 1), which can make more solvated Li ions enter inside the

electrode to enhance the electrolyte/electrode contact. Furthermore, the storage of Li in the micropores, as the covalent molecule form of Li_2, is another possible reason for the high capacity of HPCT-600-5 [30, 31]. A previous study [32] has demonstrated that the micropore size <1 nm can gather extra Li ions through a desolvation process. In this work, the micropore size is concentrated in 0.6 nm (Table 1), which may accumulate more Li ions and lead to the higher specific capacity than theoretical capacity. Although the HPCTs have great intercalation capacity for Li ions, the initial columbic efficiencies are very low in the range of 34–41% as shows in Fig. 6b. The large irreversible capacity is attributed to the formation of solid electrolyte interface (SEI) films on the surface of electrode materials, which is a common phenomenon for high specific surface area and carbonaceous materials [33]. The initial coulomb efficiency of HPCT-600-T is slightly higher than that of HPCT-600-0 and HPCT-600-10, probably owing to the low proportion of micropore specific surface area and larger micropore size (shown in Table 1). Therefore, the micropore content in the porous materials should be limited within the proper range.

Figure 6c compares the cycling performances of HPCTs at a current density of 0.1 C (1 C = 350 mA g^{-1}). After 50 cycles, the reversible capacities of HPCT-600-0, HPCT-600-2.5, HPCT-600-5, HPCT-600-2.5, HPCT-600-10 and HPCT-600-T are 233.1, 312.3, 376.9, 302.9, 242.5 and 153.6 mA g^{-1}, respectively. The reversible capacities of HPCT-600-5 are remarkably greater than those of the other composites, owing to the significantly large mesopore size, high pore volume, and the appropriate proportion of micropore and titania content. The cycling curves of HPCTs tend to be horizontal after ten cycles, indicating the superior cycling stability and reaction reversibility of the composites. The specific capacity of HPCT-600-T is 153.6 mAh g^{-1} at 0.1 C, which is consistent with the insertion coefficient (x, about 0.5 in Li_xTiO_2).

High-rate performance is one of the crucial aspects for LIBs. The rate capability of HPCTs with different contents of TiO_2 calcined at 600 °C were tested at varied current densities of 0.1, 0.5, 1 and 2 C (1 C = 350 mAh g^{-1}) for every 50 successive cycles, where the specific capacities between 40 and 50 cycles were revealed in Fig. 4d, respectively. The average discharge capacities of the HPCT composites at various current densities are distinctly higher than those of the pure titania and hierarchical porous carbon except for HPCT-10, manifesting the synergistic effects of porous carbon and titania. The discharge capacities of HPCT-600-5 maintain the highest values of 376.9 mAh g^{-1} at 0.1 C, 240.5 mAh g^{-1} at 0.5 C, 180.2 mAh g^{-1} at 1 C and 117.0 mAh g^{-1} at 2 C, respectively.

The electrochemical impedance spectroscopy (EIS) of HPCTs is measured after 50 cycles at 0.1 C, as revealed in Fig. 7. The Nyquist plots are combined with a depressed semicircle and an inclined line, representing the resistance of charge transfer through the electrode/electrolyte interface and the solid-state diffusion of Li ions in the electrode, respectively [34]. An equivalent circuit suit to the EIS of the composite is offered in the inset of Fig. 6, where R_s, R_{ct}, CPE and Z_w represent the electrolyte resistance, the charge transfer resistance, the constant phase element related to the interfacial capacitance and the Warburg diffusion impedance associated with Li ion diffusion kinetics, respectively [35]. It can be clearly

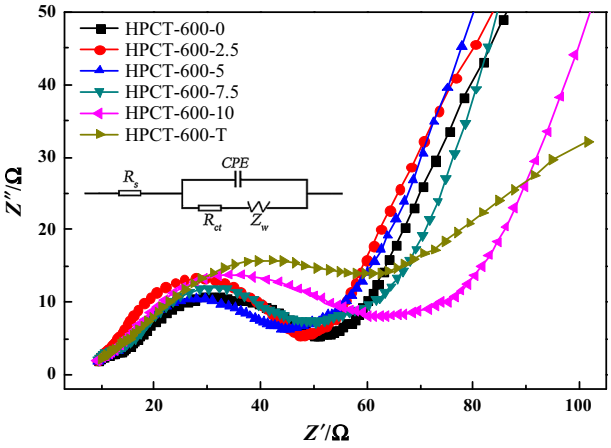

Fig. 7 EIS of HPCTs with different TiO_2 contents calcined at 600 °C

observed that the R_{ct} of HPCT-600-5 is lower than that of HPCT-600-0 and HPCT-600-T, depicting the decrease of resistance and better electrical contact between solid electrode and electrolyte. Meanwhile, the R_{ct} of HPCT-600-0 is higher than that of HPCT-600-10, ascribed to excessive TiO_2 that may enhance the resistance due to the damage of order structure of mesoporous carbon and the decrease of electrical conductivity. In addition, the slope of the curves for the HPCTs is much higher than that of the pure titania (HPCT-600-T), indicating fast Li ion diffusion kinetics, which may be ascribed to the higher surface areas to improve the contact of electrolyte and electrode.

Generally, the prepared HPCT composites manifest enhanced lithium storage properties, due to the synergistic effects of carbon and titania. The hierarchical porous carbon can efficiently improve the electronic conductivity and accelerate lithium ion diffusion. The abundant micropores and mesopores can also store extra lithium ions to enhance the specific capacity. The intrinsic structure of the titania component can also combine with lithium ions to form Li_xTiO_2. But titania has an optimum content and excess titania may block the channels of porous carbon and decrease the electrical conductivity.

Conclusions

Hierarchical porous carbon and titania composites were synthesized to be used as anode materials for LIBs. The composites with unique micropore/mesopore structure, higher specific surface and fine titania particles show high specific capacity and superior rate capability. The composite of HPCT-600-5 exhibits the highest reversible capacity of 376.9 mAh g^{-1} after 50 cycles at 0.1 C, and a capacity of 117.0 mAh g^{-1} even at 2 C. The outstanding electrochemical performances of the HPCT composites are attributed to the synergistic effects of hierarchical porous carbon and titania because of their unique structure and

component characteristics. Hierarchical porous carbon can enhance the electronic conductivity to accelerate lithium ions diffusion and increase the specific surface area to improve the wettability of the electrolyte. In addition, the hierarchical porous structure can provide a highly activated surface for the storage and fast paths for the transportation of lithium ions. Fine titania particles are well dispersed into the porous carbon, which is helpful for inhibiting the shrinkage of carbon skeleton and avoiding the agglomeration of titania during the charge and discharge process. The intrinsic structure of the titania component can also combine with lithium ions to form Li_xTiO_2. Meanwhile, controlling the proper titania content and calcination temperature are important for keeping the ordered mesoporous structure, optimum micropore/mesopore proportion and excellent electrochemical performance. These unique characteristics make the HPCT composites a promising anode and other relevant electrode materials for energy storage.

Acknowledgements This work was supported by the National Natural Science Foundation of China (Grant Nos. 51472186, 51402221).

References

1. K. Kang, Y.S. Meng, J. Breger, C.P. Grey, G. Ceder, Electrodes with high power and high capacity for recharge able lithium batteries. Science **311**, 977–980 (2006)
2. W.L. Wang, V.H. Nguyen, H.B. Gu, Favorable binding effect for improving the electrochemical performance of cobalt oxide anode for lithium ion batteries. Appl. Surf. Sci. **288**, 742–746 (2014)
3. H. Zheng, D.-Y. Park, M.-S. Kim, Preparation and characterization of anode materials using expanded graphite/pitch composite for high-power Li-ion secondary batteries. Res. Chem. Intermed. **40**, 2501–2507 (2014)
4. D. Deng, M.G. Kim, J.Y. Lee, J. Cho, Green energy storage materials: nanostructured TiO_2 and Sn-based anodes for lithium-ion batteries. Energy Environ. Sci. **2**, 818–837 (2009)
5. P.Y. Chang, C.H. Huang, R.A. Doong, Ordered mesoporous carbon-TiO_2 materials for improved electrochemical performance of lithium ion battery. Carbon **50**, 4259–4268 (2012)
6. Y.G. Wang, H.Q. Li, P. He, E. Hosono, H.S. Zhou, Nano active materials for lithium-ion batteries. Nanoscale **2**, 1294–1305 (2010)
7. H. Kim, M.G. Kim, T.J. Shin, H.J. Shin, J. Cho, TiO_2@Sn core-shell nanotubes for fast and high density Li-ion storage material. Electrochem. Commun. **10**, 1669–1672 (2008)
8. D.W. Liu, G.Z. Cao, Engineering nanostructured electrodes and fabrication of film electrodes for efficient lithium ion intercalation. Energy Environ. Sci. **3**, 1218–1237 (2010)
9. G.F. Ortiz, I. Hanzu, P. Lavela, J.L. Tirado, P. Knauth, T. Djenizian, A novel architectured negative electrode based on titania nanotube and iron oxide nanowire composites for Li-ion microbatteries. J. Mater. Chem. **20**, 4041–4046 (2010)
10. C.M. Park, W.S. Chang, H. Jung, J.H. Kim, H.J. Sohn, Nanostructured Sn/TiO_2/C composite as a high-performance anode for Li-ion batteries. Electrochem. Commun. **11**, 2165–2168 (2009)
11. Z.G. Yang, D. Choi, S. Kerisit, K.M. Rosso, D.H. Wang, J. Zhang, Nanostructures and lithium electrochemical reactivity of lithium titanites and titanium oxides: a review. J. Power Sources **192**, 588–598 (2009)
12. Y.M. Jiang, K.X. Wang, X.X. Guo, X. Wei, J.F. Wang, J.S. Chen, Mesoporous titania rods as an anode material for high performance lithium-ion batteries. J. Power Sources **214**, 298–302 (2012)
13. D. Dambournet, I. Belharouak, K. Amine, Tailored preparation methods of TiO_2 anatase, rutile, brookite: mechanism of formation and electrochemical properties. Chem. Mater. **22**, 1173–1179 (2010)
14. L.F. Shen, E. Uchaker, C.Z. Yuan, P. Nie, M. Zhang, X.G. Zhang, Three dimensional coherent titania-mesoporous carbon nanocomposite and its lithium-ion storage properties. ACS Appl. Mater. Interfaces **4**, 2985–2992 (2012)

15. X. Chen, S.S. Mao, Titanium dioxide nanomaterials: synthesis, properties, modifications and applications. Chem. Rev. **107**, 2891–2959 (2007)
16. Z. Xiu, M.H. Alfaruqi, J. Gim, J. Song, S. Kim, P.T. Duong, J.P. Baboo, V. Mathew, J. Kim, MOF-derived mesoporous anatase TiO_2 as anode material for lithium-ion batteries with high rate capability and long cycle stability. J. Alloys Compd. **674**, 174–178 (2016)
17. Z. Zhang, Z. Zhou, S. Nie, H. Wang, H. Peng, G. Li, K. Chen, Flower-like hydrogenated TiO_2(-B) nanostructures as anode materials for high-performance lithium ion batteries. J. Power Sources **267**, 388–393 (2014)
18. Y.J. Huaia, X.B. Hua, Z. Lina, Z.H. Deng, J.S. Suo, Preparation of nano-TiO_2/activated carbon composite and its electrochemical characteristics in non-aqueous electrolyte. Mater. Chem. Phys. **113**, 962–966 (2009)
19. C.J. Chen, X.L. Hu, Z.H. Wang, X.Q. Xiong, P. Hu, Y. Liu, Controllable growth of TiO_2-B nanosheet arrays on carbon nanotubes as a high-rate anode material for lithium-ion batteries. Carbon **69**, 302–310 (2014)
20. Y. Ge, H. Jiang, J. Zhu, Y. Lu, C. Chen, Y. Hu, Y. Qiu, X. Zhang, High cyclability of carbon-coated TiO_2 nanoparticles as anode for sodium-ion batteries. Electrochim. Acta **157**, 142–148 (2015)
21. J. Lee, Y.M. Chen, Y. Zhu, B.D. Vogt, Fabrication of porous carbon/TiO_2 composites through polymerization-induced phase separation and use as an anode for Na-ion batteries. ACS Appl. Mater. Interfaces **6**, 21011–21018 (2014)
22. F.H. Yang, Z. Zhang, Y. Han, K. Du, Y.Q. Lai, J. Li, TiO_2/carbon hollow spheres as anode materials for advanced sodium ion batteries. Electrochim. Acta **178**, 871–876 (2015)
23. M. Oschatz, J.T. Lee, H. Kim, W. Nichel, L. Borchardt, W.I. Cho, C. Ziegler, S. Kaskel, G. Yushin, Micro- and meso-porous carbide-derived carbon prepared by a sacrificial template method in high performance lithium sulfur battery cathodes. J. Mater. Chem. A **2**, 17649–17654 (2014)
24. J.J. Kim, H.S. Kim, J. Ahn, K.J. Lee, W.C. Yoo, Y.E. Sung, Activation of micropore-confined sulfur within hierarchical porous carbon for lithium–sulfur batteries. J. Power Sources **306**, 617–622 (2016)
25. J.T. Lee, Y. Zhao, S. Thieme, H. Kim, M. Oschatz, L. Borchatz, A.J. Silvestre, Sulfur-infiltrated micro- and meso-porous silicon carbide-derived carbon cathode for high-performance lithium sulfur batteries. Adv. Mater. **25**, 4573–4579 (2013)
26. D.W. Wang, F. Li, M. Liu, G.Q. Lu, H.M. Cheng, 3D aperiodic hierarchical porous graphitic carbon material for high-rate electrochemical capacitive energy storage. Angew. Chem. **120**, 379–382 (2008)
27. Y. Meng, D. Gu, F.Q. Zhang, Y.F. Shi, L. Cheng, D. Feng, A family of highly ordered mesoporous polymer resin and carbon structures from organic-organic self-assembly. Chem. Mater. **18**, 4447–4464 (2006)
28. J.S. Huang, B.G. Sumpter, V. Meunier, A universal model for nanoporous carbon supercapacitors applicable to diverse pore regimes, carbon materials and electrolytes. Chem. Eur. J. **14**, 6614–6626 (2008)
29. J. Chmiola, G. Yushin, Y. Gogotsi, C. Portet, P. Simon, P.L. Taberna, Anomalous increase in carbon capacitance at pore sizes less than 1 nanometer. Science **313**, 1760–1763 (2006)
30. S.-H. Yeon, W. Ahn, S. Lim, K.-H. Shin, C.-S. Jin, J.-D. Jeon, K.-B. Kim, S.B. Park, Unique cyclic performance of post-treated carbide-derived carbon as an anode electrode. Carbon **78**, 91–101 (2014)
31. K. Sato, M. Noguchi, A. Demachi, N. Oki, M. Endo, A mechanism of lithium storage in disordered carbons. Science **264**, 556–558 (1994)
32. K. Tokumitsu, H. Fujimoto, A. Mabuchi, T. Kasuh, High capacity carbon anode for Li-ion battery: a theoretical explanation. Carbon **37**, 1599–1605 (1999)
33. H. Fujimoto, Development of efficient carbon anode material for a high-power and long-life lithium ion battery. J. Power Sources **195**, 5019–5024 (2010)
34. J. Xie, X.B. Zhao, G.S. Cao, M.J. Zhao, Electrochemical performance of $CoSb_3$/MWNTs nanocomposite prepared by in situ solvothermal synthesis. Electrochim. Acta **50**, 2725–2731 (2005)
35. Y. Xia, Z. Xiao, X. Dou, H. Huang, X.H. Lu, R.J. Yan, Green and facile fabrication of hollow porous MnO/C microspheres from microalgaes for lithium-ion batteries. ACS Nano **7**, 7083–7092 (2013)